Surface Science 275 (1992) 82–91
North-Holland

surface science

Interaction of low-energy electrons and UV photons with adsorbed CF_3Cl on Pt(111)

J. Kiss [1], Diann J. Alberas and J.M. White
Department of Chemistry and Biochemistry, University of Texas, Austin, TX 78712, USA

Received 19 February 1992; accepted for publication 21 April 1992

The interaction of low energy electrons and UV photons with CF_3Cl adsorbed on Pt(111) has been studied using temperature-programmed desorption (TPD), photoelectron spectroscopy (XPS, UPS) and work-function ($\Delta\phi$) measurements. The adsorption of CF_3Cl on Pt(111) at 50 K is completely reversible. There are two distinct desorption peaks — 111–116 K (monolayer) and 82 K (multilayer). Unlike CH_3Cl, no photoeffects are observed when adsorbed CF_3 Cl is exposed to UV photons generated from a Hg arc lamp. Exposure to low energy (~ 47 eV) electrons dissociates the adsorbed molecule. The evolution of CF_3, but no CF_3Cl or Cl, occurs during irradiation. The electron-induced dissociation (EID) cross section increases with electron energy and has a threshold energy of about 12 eV. The cross section is about 7×10^{-16} cm^2 at 47 eV.

1. Introduction

The surface chemistry of alkyl halides has been studied on many metal surfaces [1–3]. The structures and bonding modes of adsorbed species are well established by different UHV surface science techniques. Besides intrinsic interest, one motivation for studying alkyl halides as precursors is motivated by their propensity to dissociate, leaving surface alkyl groups. The latter is a central concern in hydrocarbon catalysis over metals. These alkyl moieties are easily produced by photon-induced bond cleavage of C–X bonds (X = Cl, Br, I) [4–7], or by thermal decomposition of iodine containing hydrocarbons [3,8–13]. Very recently, selective C–X bond dissociation by low energy electrons has also been examined [14–15].

Here, we report on the thermal, photon and electron-driven chemistry of a fully halogenated C_1 compound, CF_3Cl, on Pt(111). The results provide an interesting contrast to data for CH_3Cl, as well as insight into certain properties of a technically relevant molecule. Fluorocarbons are important lubricants and play an important role in the etching of electronic devices. For example, reactive etching by a fluorocarbon plasma is widely used in the processing of silicon for microelectronic devices. Formation of adsorbed CF_3 and F has been reported; however, their surface chemistry is not well understood [16–18].

Very little has been published about the surface chemistry of C_1 fluorocarbons on well-characterized metal surfaces in UHV conditions. The interaction of CF_3I has been investigated on Ni(100) [19], Ru(001) [20], Ag(111) [21] and Pt(111) [22]; C–I dissociation is found in all cases.

In the present work, we turn to a less reactive fluorocarbon, CF_3Cl. It adsorbs molecularly on Pt(111) at 50 K, and there is no thermal decomposition during temperature-programmed desorption. No photoeffects are observed when adsorbed CF_3Cl is exposed to UV photons from a mercury arc lamp (energy less than 5.3 eV). Exposure to low-energy electrons (12–50 eV) does cause bond rupture. Characterization of these

[1] Permanent address: Reaction Kinetics Research Group of the Hungarian Academy of Sciences, University of Szeged, P.O. Box 105, Szeged, Hungary.

0039-6028/92/$05.00 © 1992 – Elsevier Science Publishers B.V. All rights reserved

electron-driven processes is the main focus of this paper.

2. Experimental

All experiments were carried out in a UHV chamber described elsewhere [5,23]. Briefly, the turbo-pumped chamber is equipped with XPS, UPS and TPD capabilities. A closed-cycle He cryostat (APD Cryogenics) was employed to cool the crystal to 50 K. The hemispherical electron-energy analyzer was operated at a pass energy of 40 eV for XPS and UPS. For TPD and annealing experiments, the Pt(111) sample (8 mm diameter and 2 mm thick) was heated resistively with a linear ramp (5 K/s). The sample temperature was monitored by a chromel–alumel thermocouple spot-welded to the back of the crystal. He I UPS secondary onsets were used to measure the surface work function changes ($\Delta\phi$).

A clean surface (verified by XPS) was obtained by a standard series of sputter-anneal-oxidation cycles. CF_3Cl (> 99% purity) was dosed onto the Pt(111) surface through a 2 μm pinhole doser. A linear motion drive was used to bring the end of the doser to within 2 mm of the crystal surface. This procedure minimizes adsorption on, and, in TPD, desorption from, surfaces other than the Pt(111) front face.

To investigate photon-driven chemistry, the adsorbate-covered Pt(111) surface was irradiated, using a 100 W high-pressure Hg arc lamp, from outside of the chamber through a UV grade fused quartz window. This source provides broadly distributed radiation with potential for driving photochemistry (1–5.3 eV).

For EID studies, electrons from the filament of the quadrupole mass spectrometer were utilized. As determined with the electron-energy analyzer, their average energy was 47.1 eV and the energy distribution was relatively narrow (0.6 eV FWHM). The incident electron energy was varied using a bias voltage applied between the filament and the sample. The electron flux was estimated by measuring the electron current from the sample to ground. As discussed elsewhere [24], in this configuration the current to surfaces other than the sample is negligible, but the estimate does not account for secondary electron emission and the reflection of incident electrons. Thus, the measured current is a lower limit on the actual current experienced by the adsorbate.

To minimize the effect of electron bombardment during TPD, we lowered the emission current of the mass spectrometer filament to 1 mA. Furthermore, the MS filament was switched off during adsorption. For quantitative TPD measurements, the sample was turned in front of MS when the temperature ramp reached 65 K.

3. Results and discussion

3.1. Thermal chemistry of CF_3Cl

3.1.1. TPD measurements

Fig. 1 shows TPD after dosing for various times with a fixed pressure behind the 2 μm pin

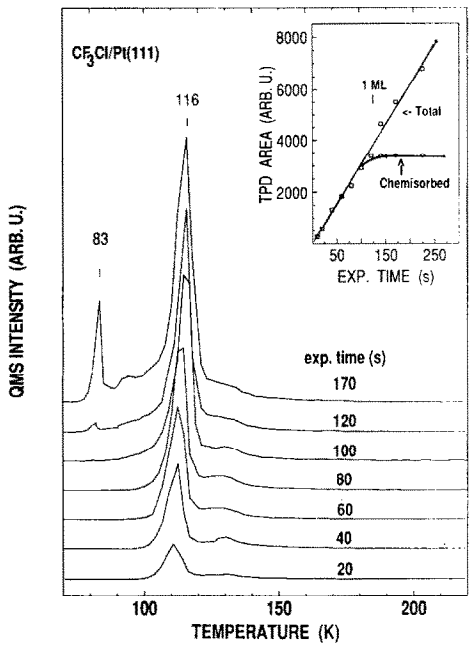

Fig. 1. TPD spectra following various exposures of CF_3Cl adsorbed on Pt(111). The dosing temperature was 50 K and the temperature ramp was 5 K/s (same in other figures). The inset shows the TPD integrated intensities as a function of increasing CF_3Cl exposure.

hole. The only observable TPD product was CF_3Cl; all the ions found tracked the parent CF_3Cl^+ peak, and the pattern was consistent with gas-phase ionization of the parent molecule. Moreover, after TPD to 250 K, the surface was clean as judged by XPS. We conclude that CF_3Cl adsorbs and desorbs reversibly. For low exposures, fig. 1 shows a single peak at 111 K which grows, moves slightly higher (116 K) and saturates at 120 s. Higher doses give a second peak at 83 K and a small feature near 95 K. As is typically done, we assign the 116 K peak to the chemisorbed monolayer and the 83 K peak to the multilayer. We did not investigate the 95 K peak. One monolayer (ML) coverage was defined as the maximum exposure that gave no multilayer peak. Consistent with the weak chemisorption bond inferred from the low desorption temperature, the shift to higher peak temperatures with exposure is taken to indicate attractive adsorbate–adsorbate interactions and two-dimensional island formation beginning at about 0.3 ML. When the monolayer state was almost saturated, the multilayer peak developed and, as expected for zero-order kinetics, this peak shifted, but very slightly, to higher temperatures with increasing exposure and was not saturable. In addition to the small 95 K peak at high exposures, *all* TPD spectra exhibit a small bump on the high-temperature side of the monolayer peak (130 K). We attribute this to desorption from defect sites. Its intensity never exceeded 5% of 1 ML.

The insert of fig. 1 shows the total TPD area and the area of the 116 K peak. Since the total area is linearly correlated with dosing time, we conclude that the sticking coefficient is constant and independent of coverage. The relatively sharp break to saturation of the 116 K (monolayer) peak indicates that a multilayer, e.g., 3D islands, TPD peak cannot be distinguished before the monolayer peak saturates.

The low and proximate TPD peak temperatures underscore the very weak bonding of CF_3Cl to Pt(111) and the small difference between the monolayer and multilayer desorption energies. The *effective* activation energy for monolayer desorption is 29 kJ/mol (calculated from the observed T_p with a pre-exponential factor of 10^{13} s^{-1}); it is 22 kJ/mol for the multilayer state (obtained from the temperature dependence of the leading edges of the desorption spectrum). These observations indicate that the CF_3Cl–Pt interaction is only slightly stronger than CF_3Cl–CF_3Cl. It is interesting that the hydrogenated C_1, CH_3Cl, also adsorbs reversibly on Pt(111) with the same monolayer (140 K)–multilayer (110 K) peak spacing, but both shifted to slightly higher temperatures [5]. These features reflect the slightly larger polarizability of CH_3Cl. Another analogous compound, CF_3I, partially decomposes on Pt(111), and, again consistent with larger polarizability, its parent desorption temperatures are higher and more widely separated (168 K for the monolayer and 100 K for the multilayer) [22].

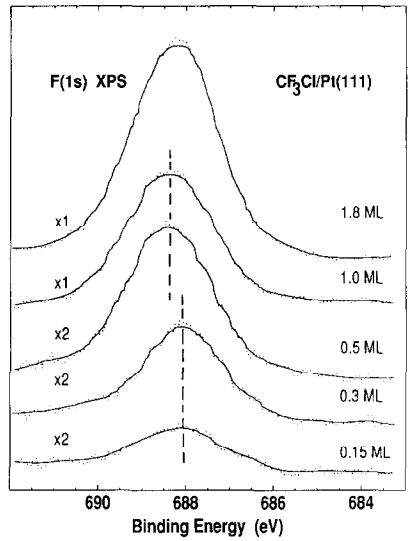

Fig. 2. F(1s) XPS of CF_3Cl adsorbed on Pt(111) at 50 K for various coverages (0.15–1.8 ML). The solid line is a Fourier smoothed version of the raw data (dots). The vertical dashed lines are located at 688.1 and 688.4 eV.

3.1.2. XPS, UPS and $\Delta\phi$ measurements

The F(1s) spectra for several coverages are shown in fig. 2. At low coverages (< 0.3 ML), there is a peak at 688.1 eV (FWHM = 1.9 eV). With increasing coverage to 1.8 ML, the F(1s) signal intensifies, broadens on the high BE side to 2.1 eV FWHM, and the peak shifts to 688.4 eV. Because of the width, we interpret these

spectra in terms of at least two chemical environments and fit them with 2 Gaussian peaks, centered at 687.8 and 688.6 eV. We propose that the lower binding-energy peak represents molecules with F atoms closer to the metal, where final-state screening is greater. The intensity of the higher binding-energy peak increases with the coverage. Their ratio is about 2:1 at 1 ML coverage.

The Cl(2p) XPS for adsorbed CF_3Cl shows coverage independent (0–1 ML) features at 200.7 eV and at 202.0 eV, the widths of which do not change (see fig. 6 for 1 ML case). The two peaks originate from the two spin–orbit states of a single chemical species. The peaks shift to higher BE in the multilayer.

When the adsorbate-covered surface was heated to 200 K, both F(1s) and Cl(2p) signals disappeared, consistent with non-dissociative adsorption and TPD. This contrasts with CF_3I, where partial dissociation occurs below 135 K and the F(1s) moves to 685.8 eV, indicating the formation of Pt–CF_3 bonds [22]. It is also interesting that the F(1s) and Cl(2p) XPS signals for CF_3Cl are at higher BE (by about 0.8 eV) than the analogous signals from adsorbed CF_3I and CH_3Cl. This is consistent with the relatively weak interaction between CF_3Cl and the surface.

The valence orbitals of adsorbed CF_3Cl are characterized by three main He I UPS peaks (fig. 3). Taking into account the gas phase spectra of CF_3Cl [25a], we assigned the 6.5, 9.5 and 10.9 eV peaks (below the Fermi level) as emissions from the chlorine lone pair, C–Cl bond, and C–F bond (including F lone pair), respectively. The relatively weak feature near 15 eV probably contains a F(2p) character [25b]. It is noteworthy that the peak positions shift between 1.0 and 1.8 ML, consistent with a surface structure in which the first layer saturates before 3D structures begin to form. Comparing with CH_3Cl, which shows the chlorine lone pair at 5.3 eV and C–Cl bond around 8.3 eV, it is more difficult to ionize CF_3Cl because fluorine substitution stabilizes these orbitals. This UPS data is useful for interpreting the electron-induced chemistry discussed below.

The work-function change ($\Delta\phi$) with increasing exposure (fig. 4) is striking, and differs strongly from that characteristic of CH_3Cl or CF_3I measured on the same sample at 50 K. Up to 0.3 ML CF_3Cl, $\Delta\phi$ is below detection limits (< 0.05 eV). Above this coverage, $\Delta\phi$ drops slightly but is less than 0.1 eV at 1 ML. CH_3Cl and CF_3I are very different — $\Delta\phi$ drops sharply, by as much as 1.2

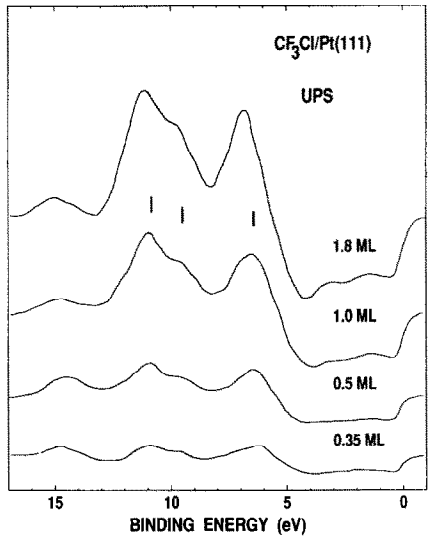

Fig. 3. He I UPS (difference spectra) of CF_3Cl adsorbed on Pt(111) at 50 K for various coverages (0.35–1.8 ML). Vertical bars mark the expected positions of molecular orbital ionizations in CF_3Cl (see text).

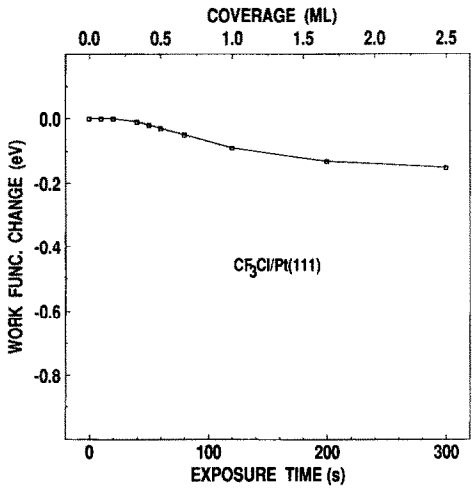

Fig. 4. $\Delta\phi$, determined from UPS thresholds, as a function of CF_3Cl coverage (upper scale) and exposure (lower scale) at 50 K.

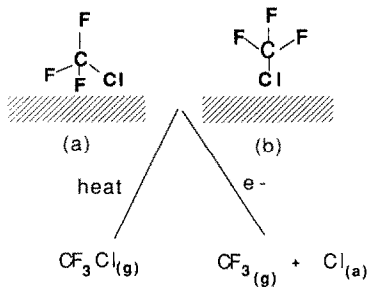

Scheme 1. Possible arrangements of adsorbed CF_3Cl on Pt(111) and the response the thermal and electron activation.

eV over the first ML [5]. This is generally observed for monohalogenated C_1 molecules and indicates that they bond with the polarizable halogen towards the surface and the positive end of their permanent dipole pointed towards the vacuum [1,3,9,26,27]. To explain why CF_3Cl is so different, we have to consider both the permanent dipole moment (0.5 D) and the polarizability, both of which are small. Furthermore, the direction of the permanent dipole (negative end points in the direction of the fluorines) and the polarizability (Cl end) are oriented such that they will tend to compensate each other, i.e., if the polarizability of the Cl lone pair provides an attractive interaction orienting the CF_3Cl with the Cl towards the metal, then the permanent dipole will tend to compensate the induced dipole because its negative end will be outward. We believe that CF_3Cl slightly prefers to adsorb via chlorine as in the case of chloromethanes, but as shown in scheme 1, at least for low coverages, the CF_3 group is inclined to the surface and one or two fluorines are close to the metal. Adsorption of CF_3Cl on graphite via chlorine was also assumed in beam–surface scattering experiments [28].

3.2. Interaction with photons

The TPD spectra of 1 ML CF_3Cl before and after UV photon irradiation with the unfiltered Hg arc lamp were identical. No decomposition products were observed in TPD after irradiation at 50 K. Similarly, the XPS peak intensities and position for F(1s) and Cl(2p) did not change after photon irradiation. We conclude that, unlike CH_3Cl [6,7], photons with energies below 5.3 eV (> 230 nm which is the onset of the Hg arc lamp) cause neither desorption nor photodissociation of CF_3Cl.

Gas-phase CF_3Cl is transparent to photons with the energies used here. Below 180 nm, a valence-shell, $n \rightarrow \sigma^*$ transition, in which one of the electrons of the chlorine lone pair is raised to an antibonding orbital in the C–Cl bond, occurs in a broad band centered at about 140 nm [29]. In view of the very weak perturbation by the surface, and our experience with other systems, we rule out direct photon absorption by the adsorbate as a potentially relevant excitation mechanism.

Photon-induced electron transfer processes, e.g., photoelectron attachment, play an important role in the photoinduced dissociation of CH_3Cl adsorbed on Pt(111) [5]. Such attachment, with a threshold around 1 eV and a maximum at 1.4 eV, has been reported for gas phase CF_3Cl [31]. For adsorbed CF_3Cl on Pt(111), the work function, even at 1 ML coverage, is 5.6–5.7 eV. Thus, electrons, to be effective, must tunnel into CF_3Cl since in our set-up, the maximum photon energy is 5.3 eV. For CH_3Cl, this does not occur with measurable probability; only when the work function drops below the photon energy and free electrons in vacuum are observed does the photon-driven C–Cl bond cleavage occur [5]. We conclude that, if electrons do tunnel into adsorbed $CF_3Cl(a)$, they do not promote any chemistry.

3.3. Interaction with low-energy electrons

Since neither photons nor hot subvacuum level-charge carriers are effective in the CF_3Cl/Pt(111) system, we turn to low-energy electrons (12–50 eV) and, indeed, observe strong electron-induced dissociation (EID) in the adsorbed layer at 50 K. As indicated in scheme 1, we find strong evidence for the desorption of CF_3 and the retention of Cl.

Fig. 5 shows the F(1s) XPS peak after exposing 1 ML CF_3Cl to 47.1 eV electrons (flux = 7.5×10^{12} electrons cm^{-2} s^{-1}). As the electron exposure time increases, the F(1s) peak area decreases,

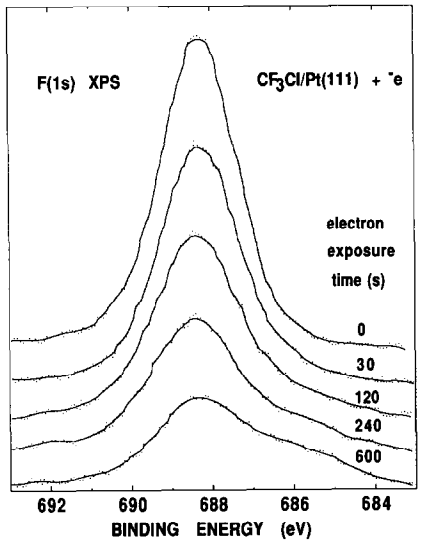

Fig. 5. F(1s) XPS of 1 ML of CF_3Cl adsorbed on Pt(111) at 50 K as a function of electron irradiation time (flux $= 7.5 \times 10^{12}$ electrons cm^{-2} s^{-1}).

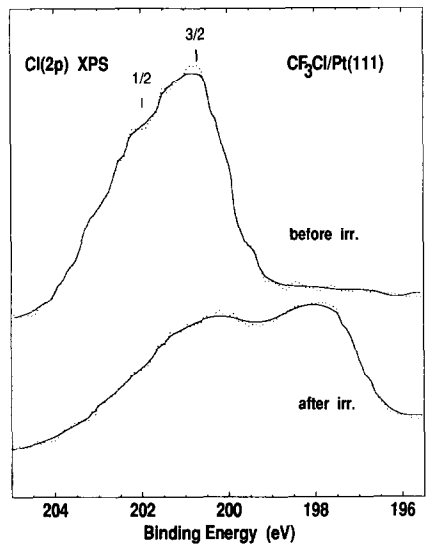

Fig. 6. Cl(2p) XPS of 1 ML of CF_3Cl adsorbed on Pt(111) before and after 240 s electron irradiation (flux $= 7.5 \times 10^{12}$ electrons cm^{-2} s^{-1}).

indicating electron-driven desorption of fluorine-containing species. Above 120 s, the peak slightly broadens towards the lower BE side.

Fig. 6 shows companion Cl(2p) signals before and after 240 s electron exposure. The $Cl(2p_{1/2})$ BE shifts from 200.7 eV to 197.9 eV with electron dose. In contrast to F(1s), the Cl(2p) peak area decreases by no more than 5% after 240 s electron exposure; within experimental error there is no electron stimulated desorption (ESD) of Cl-containing species.

To confirm the loss of F-containing species, we monitored the desorption of products during electron beam exposure; only CF_3 radicals were detected in the gas phase. There were no signals for CF_3Cl or Cl. Fig. 7 shows an isothermal desorption spectrum for CF_3 during exposure of 1 ML CF_3Cl to 47.1 eV electrons (flux $= 5.6 \times 10^{12}$ electrons cm^{-2} s^{-1}) at 50 K. Before starting the electron irradiation, the sample was turned away from the QMS filament. To start the irradiation, the sample was turned toward the filament; the intensity of CF_3 (monitored at 69 and 50 amu) promptly increased and then decreased with irradiation time. At 180 s, the sample was negatively biased by 50 eV, and the signal immediately disappeared. When the bias was removed, the formation of CF_3 promptly took up where it left off. This result indicates that the CF_3 signal is due to an electron-induced reaction on the surface.

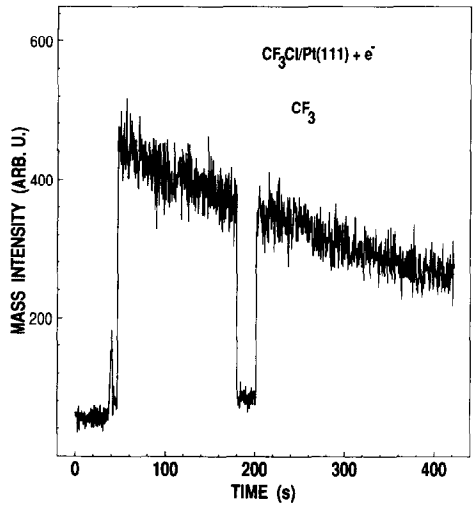

Fig. 7. CF_3^+ signal during electron irradiation of 1 ML of CF_3Cl (flux $= 5.6 \times 10^{12}$ electrons cm^{-2} s^{-1}). The sample was biased negatively at 180 s (see text).

The time-dependent loss of parent molecule during irradiation, as determined by TPD, can be used as the most quantitative measure of the electron-driven processes. Fig. 8 shows the TPD spectra of molecular CF_3Cl taken after electron irradiation (47.1 eV) of 1 ML for various times. The CF_3Cl TPD peak area, like the F(1s) XPS area, decreases monotonically with increasing electron fluence. The inset of fig. 8 shows a semi-logarithmic plot of the fractional decrease in CF_3Cl peak area as a function of electron fluence. The slope of this plot is related to the EID cross section, σ, according to

$$\ln(I(t)/I(0)) = -(i_e t/eA) = -F_e\sigma,$$

where t is the irradiation time, i_e is the electron current, e is the electron charge, A is the surface area, and F_e is the electron fluence. The total cross section was calculated from the slope of this curve. We estimated an EID cross section of 7×10^{-16} cm^2. This value must be considered an upper limit because, as mentioned earlier, the scattered primary and secondary electron fluences are not taken into account in this calculation. For large electron fluences ($> 18 \times 10^{14}$ electrons cm^{-2}), the slope is less steep, probably because newly formed adsorbed species, e.g., Cl, inhibit the EID process.

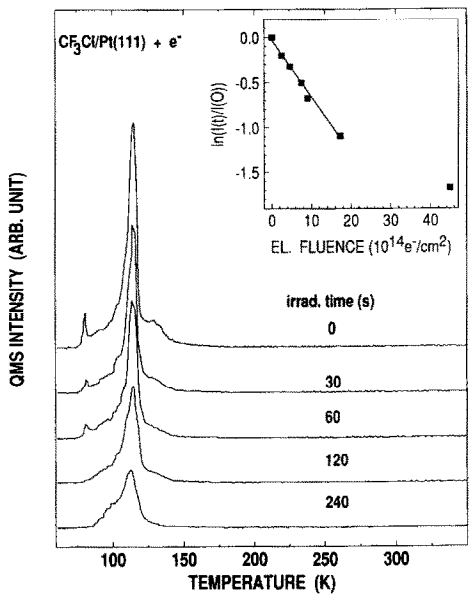

Fig. 8. TPD spectra for 1 ML CF_3Cl adsorbed on Pt(111) as a function of increasing irradiation time (flux = 7.5×10^{12} electrons cm^{-2} s^{-1}). The inset shows the semi-logarithmic plot of the CF_3Cl TPD area as a function of electron fluence.

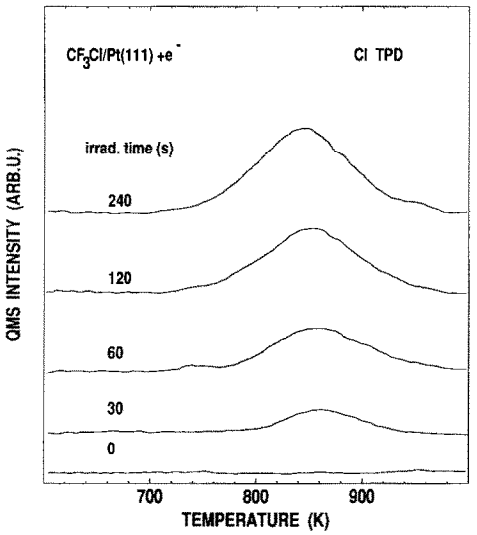

Fig. 9. TPD spectra of chlorine formed during electron irradiation of CF_3Cl adsorbed on Pt(111).

According to XPS, Cl is not lost during electron beam dosing. In TPD, as expected, atomic chlorine was observed at high temperatures (fig. 9), with a peak at 850 K, as observed after photoinduced decomposition of CH_3Cl or $BrCH_2CH_2Cl$ [5,32]. The desorbed amount increases with electron exposure (the fluence is the same as in fig. 8). For high electron exposures (600 s), HCl desorption (fig. 10) was observed at 257 K, indicating reaction of Cl with H adsorbed from background H_2.

For 120 s or longer exposures of 1 ML CF_3Cl to 47.1 eV electrons (flux = 7.5×10^{12} electrons cm^{-2} s^{-1}), some fluorine-containing moieties remain on the surface and desorb during thermal desorption. Fig. 10 shows the results following 600 s irradiation time. A small amount of parent desorbed with the same TPD shape as the 240 s curve of fig. 8 (i.e., peak at 110 K). Contributions of parent cracking to 50 and 69 amu have been subtracted from the CF_3 and CF_2 signals in fig. 10. CF_3 (69 amu) radical desorption was observed between 380 and 560 K. Some HF desorbs in two

peaks, 154 and 270 K. It is likely that the adsorbed F atom reacts with adsorbed background hydrogen in this process.

The CF_2 (50 amu) radical desorption was found at 157 K. In the new data, it appears as a growing shoulder on the high-temperature side of the parent desorption signal. There is no analogous shoulder for CF_3^+. In addition to these products, some CF_3 reacts with background hydrogen and desorbs as CF_3H at 144 K.

To determine whether the CF_x fragments form during irradiation at 50 K or during TPD of CF_3 formed by electron irradiation, we examine the XPS results (fig. 5). Above 240 s irradiation time, the F(1s) peak is significantly broadened to low BE. For peak synthesis, we used a peak position of 685.8 eV with 1.9 eV FWHM to characterize adsorbed CF_3 radical on Pt(111) [22], and peak position of F(1s) (688.4 eV) which corresponds to the remaining parent CF_3Cl. The F(1s) peak cannot be reasonably fit to a sum of these two separate components, and we suppose that some lower BE species, e.g., CF_2 and F, are formed during extended electron irradiation. The amounts of retained CF_3, CF_2 and F are small compared to the CF_3, which desorbs during electron irradiation. Taking into account the XPS areas before and after irradiation, 85% of the CF_3 desorbs and 15% remains, some of which decomposes further.

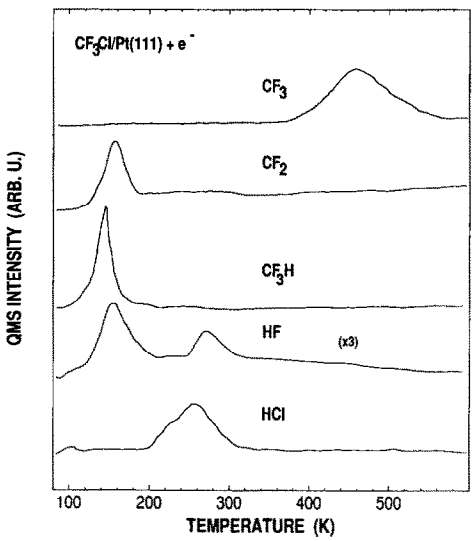

Fig. 10. Post-irradiation TPD profiles for CF_3, CF_2, CF_3H, HF and HCl after 600 s electron irradiation of CF_3Cl adsorbed on Pt(111). Electron flux is 7.5×10^{12} electrons cm^{-2}. CF_2^+ contribution from CF_3 has been subtracted from the reported CF_2 signal.

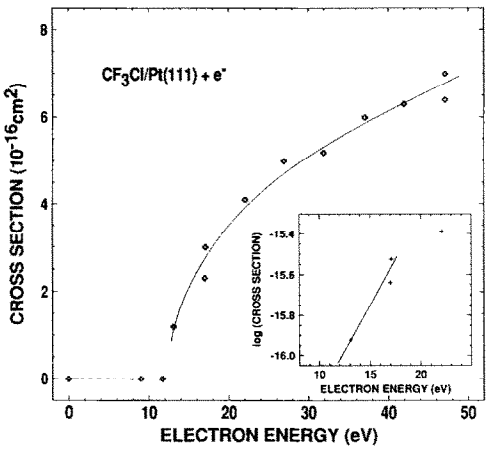

Fig. 11. Electron-energy dependence, based on post-irradiation TPD, for EID cross section of 1 ML of CF_3Cl. The insert shows a semilogarithmic plot of the cross section near threshold.

The electron-energy dependence is interesting and is summarized in fig. 11. At 0 eV there is no current and, as required, no cross section (confirming the absence of certain artifacts). For two energies ($\sim$ 9 and 12 eV), there is plenty of current, but still no cross section. Above 12 eV, the cross section suddenly increases and, by the extrapolation in the inset, we estimate a threshold between 11.5 and 12.0 eV.

Electrons interact with molecules in several manners. Low-energy electron processes generally involve electron capture and the formation of transient negative ion species. For higher energies, electrons ionize the molecule by core or valence electron ejection, resulting in a positive ion. Electron excitation from one of the occupied levels to one of the unoccupied levels within the molecule is also possible. All these excitation processes may lead to dissociation.

The extrapolated threshold, 11.5–12 eV, is very close to the first gas-phase ionization potential of CF_3Cl, 13.0 eV [29]. This ionization potential is connected with the chlorine lone-pair electrons.

When CF_3Cl is adsorbed on Pt(111), we measured this orbital in UPS peaking at 6.5 eV (threshold ~1 eV lower) below the Fermi level at 1 ML, a reasonable position for an ionization threshold and, thus, a desorption threshold of 12 eV. It is reasonable to assert that the EID process involves ionization of CF_3Cl and that it involves the lone pair. Toward higher energies, other ionizations may be involved; for example, the second ionization potential for CF_3Cl, an orbital with considerable C–Cl character, occurs at 15 eV in the gas phase. This orbital is detected at 9.5 eV (below the Fermi level) in UPS of adsorbed CF_3Cl (fig. 3).

Assuming ionization occurs, a short-lived positive ion will be formed. Fragmentation in the gas phase is facile and we presume the same sort of C–Cl rupture leads to CF_3 desorption. If quenching occurs after sufficient time, dissociation can occur from the ground state. Empirically, most of the CF_3 formed has sufficient translational energy to escape the surface during electron irradiation.

4. Summary and conclusion

The work reported here can be summarized as follows:

(1) The adsorption of CF_3Cl on Pt(111) is completely reversible with desorption peaks at 116 and 82 K for monolayer and multilayer, respectively.

(2) Due to a small permanent dipole and to the polarizability of the molecule, which tend to compensate each other, there is a negligible $\Delta\phi$ during adsorption. The adsorbed molecules have a tendency to form islands due to attractive interaction between adsorbates.

(3) No photoeffects were observed when adsorbed CF_3Cl was exposed to UV photons with energies of 5.3 eV or less.

(4) Exposure to electrons results in decomposition of the adsorbed molecules. The desorption of CF_3 during irradiation is readily monitored. There is no electron-stimulated desorption of molecular CF_3Cl or atomic Cl.

(5) The initial electron induced dissociation cross section for 1 ML of CF_3Cl is about 7×10^{-16} cm^2 at 47.1 eV. It has a threshold between 11.5 and 12.0 eV. The EID process can be ascribed to the formation of a short-lived positive ion, which either dissociates directly to CF_3 and Cl, or is quenched to a vibrationally hot (activated) state that dissociates.

Acknowledgement

This work was supported in part by the National Science Foundation, Grant CHE9015600.

References

[1] M.A. Henderson, G.E. Mitchell and J.M. White, Surf. Sci. 184 (1987) L325.
[2] K.G. Lloyd, B. Roop, A. Campion and J.M. White, Surf. Sci. 214 (1989) 227.
[3] F. Zaera, Acc. Chem. Res., in press, and references therein.
[4] B. Roop, S.A. Costello, Z.-M. Liu and J.M. White, Springer Series in Surface Science, Vol. 14, Solvay Conference on Surface Science, Ed. F.W. de Wette (Springer, New York, 1988) p. 343.
[5] S.K. Jo, X.-Y Zhu, D. Lennon and J.M. White, Surf. Sci. 241 (1991) 231.
[6] X.-L. Zhou, X.-Y. Zhu and J.M. White, Acc. Chem. Res. 23 (1990) 327, and references therein.
[7] X.-L. Zhou, X.-Zhu and J.M. White, Surf. Sci. Rep. 13 (1991) 77, and references therein.
[8] (a) M.A. Henderson, G.E. Mitchell and J.M. White, Surf. Sci. 248 (1991) 279;
(b) X.-L. Zhou and J.M. White, J. Phys. Chem. 95 (1991) 95.
[9] F. Zaera, Surf. Sci. 219 (1989) 453.
[10] C.J. Jenks, C.-M. Chiang and B.E. Bent, J. Am. Chem. Soc. 113 (1991) 6308.
[11] F. Solymosi and K. Revesz, J. Am. Chem. Soc. 113 (1991) 9145.
[12] Z.-M. Liu, X.-L. Zhou, D.A. Buchanan, J. Kiss and J.M. White, J. Am. Chem. Soc. 114 (1992) 2032.
[13] B.E. Bent, R.G. Nuzzo, B.R. Zegarski and L.H. Dubois, J. Am. Chem. Soc. 113 (1991) 1137; 1143.
[14] X.-L. Zhou, P.M. Blass, B.E. Koel and J.M. White, Surf. Sci. 271 (1992) 452.
[15] X.-L. Zhou and J.M. White, J. Chem. Phys. 92 (1990) 5612.
[16] B. Roop, S. Joyce, J. Schultz and J. Steinfeld, J. Chem. Phys. 83 (1985) 6012.

[17] R.M. Robertson, D.M. Golden and M.J. Rossi, J. Vac. Sci. Technol. B 6 (1988) 1632.
[18] W.R. Creasy and S.W. McElvany, Surf. Sci. 201 (1988) 59.
[19] R.G. Jones and N.K. Singh, Vacuum 38 (1988) 213.
[20] J.S. Dyer and P.A. Thiel, Surf. Sci. 238 (1990) 179.
[21] M.E. Castro, L.A. Pressley, J. Kiss, S.K. Jo, X.-L. Zhou and J.M. White, to be published.
[22] Z.-M. Liu, X.-L. Zhou, J. Kiss and J.M. White, to be published.
[23] J. Kiss, D. Lennon, S.K. Jo and J.M. White, J. Phys. Chem. 95 (1991) 8054.
[24] X.-L. Zhou, M.E. Castro and J.M. White, Surf. Sci. 238 (1990) 215.
[25] (a) J. Doucet, P. Sauvageau and C. Sandorfy, J. Chem. Phys. 58 (1973) 3708;
(b) B.W. Yates, K.H. Tau and G.M. Bancroft, J. Chem. Phys. 85 (1986) 3840.
[26] R.G. Nuzzo and L.H. Dubois, J. Am. Chem. Soc. 108 (1986) 2881.
[27] J.G. Chen, T.B. Beebe, Jr., J.E. Crowell and J.T. Yates, Jr., J. Am. Chem. Soc. 109 (1987) 1726.
[28] R.S. Mackay, T.J. Curtiss and R.B. Berstein, Chem. Lett. 164 (1989) 341.
[29] C. Sandorfy, Atmos. Environ. 10 (1976) 343.
[30] D.E. Robins, Geophys. Res. Lett. 3 (1976) 213.
[31] D.L. McCorkle, A.A. Christodoulides, L.G. Christophorou and I. Szamrej, J. Chem. Phys. 72 (1980) 4049.
[32] S.K. Jo and J.M. White, Surf. Sci. 245 (1991) 305.